On the Origin of Low Frequency Pressure Fluctuations in Passenger Compartments of Vehicles

Laura Breitenbücher, Dr.-Ing. Matthias Lang, Dr.-Ing. Maarten Brink, Dr.-Ing. Thomas Wiegand, Prof. Dr.-Ing. Andreas Wagner
Dr. Ing. h.c. F. Porsche AG
Porschestraße 911
71287 Weissach

laura.breitenbuecher1@porsche.de
andreas.wagner@ifs.uni-stuttgart.de

Abstract: Aeroacoustics have become increasingly important as they significantly determine comfort in passenger compartments.
Electric vehicles typically feature an underbody designed to minimize drag. The aerodynamic design also contributes to a reduction in acoustic interference. However, low frequency pressure fluctuations with significant amplitudes in the range of 30 Hz have been observed as a result of the optimization. Time-resolved Particle Image Velocimetry (PIV) measurements in the flow field beneath the car already showed periodical structures around the dominant frequency.
The aim of this study is to show the correlation between flow characteristics and low-frequency pressure fluctuations in the interior. A mobile measurement system was established to simultaneously acquire acoustic data and velocity fluctuations near the underbody using hot-wire anemometry. Direct online processing of both data streams enables a precise quantification of the mathematical correlation between acoustic and aerodynamic signals. Relevant flow phenomena were detected beneath the vehicle by pointwise traversing the hot-wire probe. Additionally, visualizations of the wall shear pattern along the underbody showed a strong correlation with measured results and provided further insights into the underlying flow physics.
It is demonstrated that a combined application of quantitative and qualitative experimental techniques, as well as simulations, provides a deeper insight into the underlying mechanisms, thereby enhancing the understanding of the complex flow field. Finally, this approach facilitated the development of countermeasures in the early stages of development, reducing the need for unplanned optimization loops.

Contribution: 2025 FKFS Conference on Vehicle Aerodynamics and Thermal Management
15 – 16 October 2025 | Leinfelden-Echterdingen

1 Introduction

Customers' expectations of the driving experience in the interior of a vehicle are becoming increasingly important. Battery electric vehicles (BEVs) generate almost no drive noise and there are no combustion masking effects either. As a result, flow noise becomes relevant at lower speeds. [1] Due to the absence of an exhaust system and advantages regarding drag coefficients, BEVs typically have a very streamlined underbody. This underbody shape is generally characterized by a low acoustic disturbance potential. However, low-frequency pulsations in the frequency range below 20 Hz have been observed in certain prototypes of battery electric vehicles. These strong pressure fluctuations excite the vehicle's interior through the air path of the ventilation exits in the rear area. As a result, uncomfortable pressure fluctuations occur in the vehicle interior, leading to a reduction in passenger comfort. In this study, this phenomenon is referred to as “underbody buffeting.”

Previous investigations have shown that the flow phenomenon is very sensitive to geometric modifications on the vehicle’s underbody. However, even small modifications can influence not only the aeroacoustics but also the aerodynamics of the vehicle. [2, 3, 4]

In [2], Weber identified high-energy separations at the front wheel spoilers and at the front wheels as the cause of the high-pressure fluctuations in the rear area of the vehicle. The underbody buffeting can be generated at a generic car reference model. This was demonstrated in [4], where investigations were conducted both in CFD-simulations and in the wind tunnel. In order to identify the exact formation mechanism of the underbody buffeting, time-resolved Particle Image Velocimetry (PIV) measurements were carried out in the model wind tunnel of the Research Institute for Automotive Engineering and Powertrain Systems Stuttgart (FKFS). [5]

In addition to analysing the mean and instantaneous velocity, the velocity fluctuations were subsequently investigated. The Ω-method was employed for the identification and visualization of vortices. [6] The Spectral Proper Orthogonal Decomposition (SPOD) method was applied to identify coherent structures. [7]

The dominant frequency that can be perceived in the interior could be detected by PIV measurements in the flow. [5] This paper presents supplementary hot-wire and microphone measurements as well as visualizations that offer deeper insight into the fundamental mechanism primarily responsible for underbody buffeting. It will be demonstrated that combining the strengths of these various quantitative and qualitative techniques yields results unattainable by applying any single method alone. A transient measurement system is being developed to detect acoustically relevant flow structures, utilizing real-time online evaluation. Through signal correlation, the system aims to establish a direct relationship between measured flow fluctuations and their effects on acoustics. The measurement system is intended to be relatively cost-effective, quick, and mobile. The critical areas identified through hot-wire and microphone coherence will subsequently be compared with the flow structures using flow visualization techniques. Finally, the findings from the investigations will be utilized to develop appropriate countermeasures.

2 Method

All investigations in this study were carried out in the model wind tunnel of the FKFS. The measurements were performed using a generic vehicle reference model based on the SAE-Body defined by the SAE committee, scaled at 1:4 [8]. This setup enables the isolation of flow phenomena by eliminating additional aeroacoustics noise sources and related interference effects. Unlike the original model with a smooth underbody, the current model includes wheel arches and wheels. Moreover, various wheel spoilers and add-on components can be attached to the vehicle's underbody. Figure 1 shows the model in the wind tunnel.

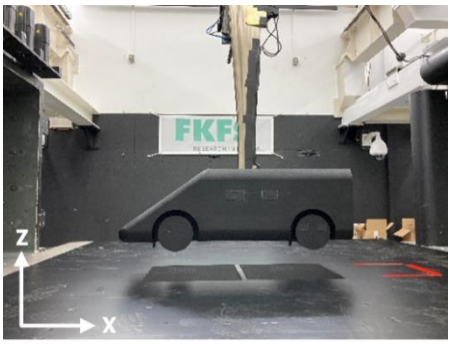

Figure 1: Geometry of the SAE-Body with wheels and wheel spoilers

It has been demonstrated that applying PIV enables the detection of flow structures associated with low-frequency phenomena within the flow field [5]. While PIV provides valuable imaging data, its setup and data postprocessing require a comparatively high time investment. Consequently, the relationship between velocity fluctuations and their acoustic feedback is not immediately accessible during the measurements.

To reduce measurement time and improve efficiency during the development of countermeasures in such measurement campaigns, a new measurement system has been set up. The schematic setup of this system is shown in Figure 2. It allows for the simultaneous acquisition of time-resolved signals with one microphone, two pressure transducers, and a single hot-wire probe. Additionally, a traverse system can be connected to acquire time series of pressure or velocity automatically within the flow field.

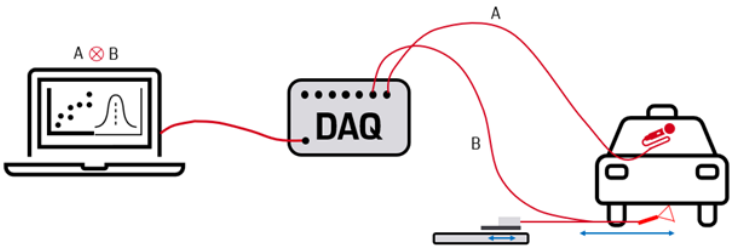

Figure 2: Schematic setup of the measurement system with hot-wire and microphone

A custom-developed software enables real-time processing of signals acquired from a continuous data stream. Frequency spectra and the coherence between two selected signals are computed and displayed immediately. The coherence function, calculated as described in [9], quantifies the correlation between two signals across different frequencies. In other words, it indicates the strength of the connection or any linear dependency between the signals in the frequency domain. This system allows for scanning of the flow field to identify regions where velocity fluctuations correlate strongly with acoustic frequencies, thereby pinpointing flow areas with coherent structures directly related to aeroacoustics phenomena. In the present study, signals from the microphone and hot-wire probe were analysed to precisely quantify the mathematical correlation between acoustic and aerodynamic phenomena while moving the hot-wire probe beneath the car model along the y-axis. The microphone was positioned inside the model, specifically within the passenger compartment. For direct comparison with PIV measurements [5], the z-position of the hot-wire probe was selected to match the height of the PIV light sheet.

Another classical method applied is the kerosene soot technique, which is used to visualize the direction of wall shear stress. In contrast to the traditional approach, a mixture of paraffin oil and coloured particles was employed. The components of this mixture were selected so that its viscosity, combined with the wall shear stress, permits a certain movement of the liquid, thereby revealing the resulting flow structures. The substance was applied to the underside of the SAE-Body, and the model was subjected to the same flow conditions as during the PIV and aeroacoustics measurements. While the direction of the shear stress indicates the orientation of the wall streamlines, the concentration of the liquid after the experiments serves as an indicator of the wall shear of the flow velocity.

3 Results

In this chapter, the results of three different configurations are presented. Figure 3 shows the frequency spectra of the considered variants. These spectra were derived from pressure fluctuations measured with surface microphones positioned in the rear area of the vehicle's underbody. The configuration *with_WS* features wheel spoilers in front of the wheels. The dominant peak around 90 Hz in the frequency spectrum clearly indicates a strong occurrence of underbody buffeting. In the configuration without wheel spoilers (*without_WS*), the wheel spoilers were removed, and underbody buffeting does not occur. For the configuration *with_VG*, a forward-facing vortex generator was installed at the inner edge of the wheel spoiler, which significantly reduces underbody buffeting.

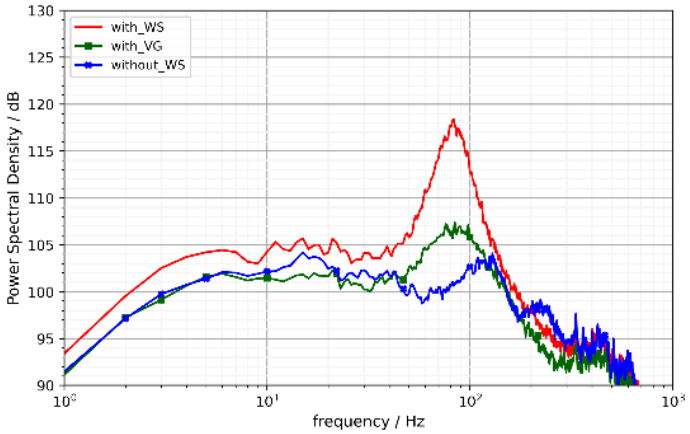

Figure 3: Frequency spectra of configurations *with_WS* (with front wheel spoiler), *with_VG* (with vortex generator) and *without_WS* (without front wheel spoiler) measured with a microphone in the diffusor area of the vehicle

3.1 Configuration with wheel spoiler

In the following, the configuration with front wheel spoilers *with_WS*, where underbody buffeting occurs, will be discussed.

Previous studies using PIV measurements have provided detailed insights into the underlying flow. In this context, SPOD analysis was employed to identify coherent structures within the flow. Figure 4 presents the SPOD spectrum and the first SPOD mode at 78 Hz.

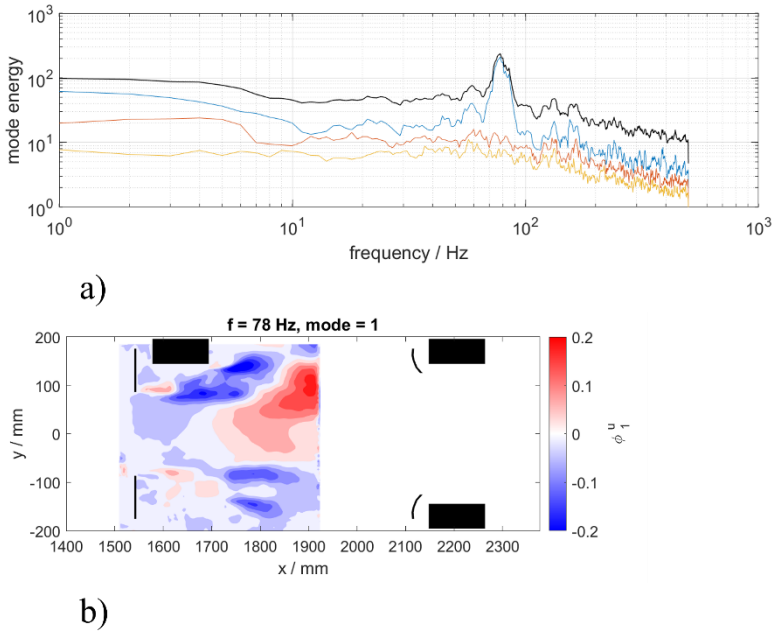

Figure 4: a) SPOD spectra and b) first SPOD mode of configuration *with_WS*

The investigation reveals that the coherent structures primarily originate at the inner edge of the wheel spoiler. Furthermore, it is evident that fluctuations in flow parameters occur within the shear layer behind the wake of the wheel spoiler.

Hot-wire measurements were performed at selected positions along the x-direction (wind direction) to capture velocity fluctuations beneath the model. The hot-wire probe was traversed along the y-direction. Figure 5 shows profiles of the mean velocity and standard deviation derived from the hot-wire signals across the vehicle width in the y-direction for all three configurations. In this section, configuration *with_WS* (red lines) is considered. The shear layer is located within the range of - 100 mm < y < - 60 mm, indicated by the strong velocity gradient. A high standard deviation level indicates significant flow fluctuations, with the maximum standard deviation occurring at approximately y ≈ -100 mm, as shown in Figure 5b).

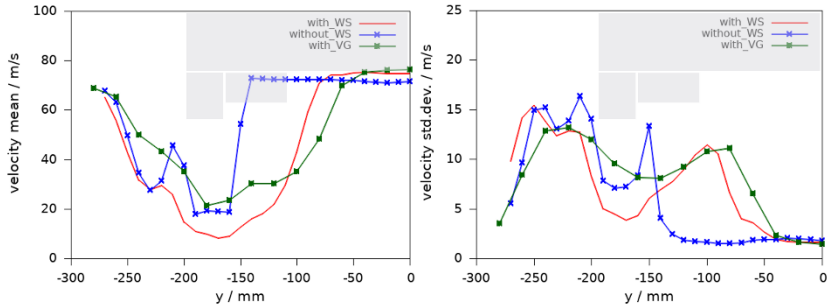

Figure 5: a) Mean velocity and b) standard deviation of measured velocity profiles across the vehicle width of configurations *with_WS*, *without_WS* and *with_VG*

Shear layers are regions characterized by a strong velocity gradient between two fluid layers. They exhibit high instability with significant disturbance growth, resulting in pronounced velocity fluctuations. Figure 6a) shows the 1/3 octave sound pressure level frequency spectra. The solid lines represent the measurement from the microphone inside the vehicle cabin, while the dashed lines correspond to the hot-wire signal at y = -80 mm within the shear layer. Although expressing velocities in decibels is not strictly physically accurate, we use this approach to enable a direct comparison with acoustic quantities. The coherence functions between these two signals are presented in Figure 6b).

For configuration *with_WS* in the region of strong disturbance growth, prior to saturation, the fluctuations are confined to a dominant frequency range (here 55 Hz < f < 110 Hz). As shown in Figure 6b), the coherence between the hot-wire and microphone signals exhibits a pronounced peak within this frequency range, corresponding to the underbody buffeting. This peak indicates a strong correlation between the velocity fluctuations within the shear layer beneath the model and the acoustic phenomena measured in the passenger compartment. These findings suggest that the flow structures developing in this shear layer are acoustically significant.

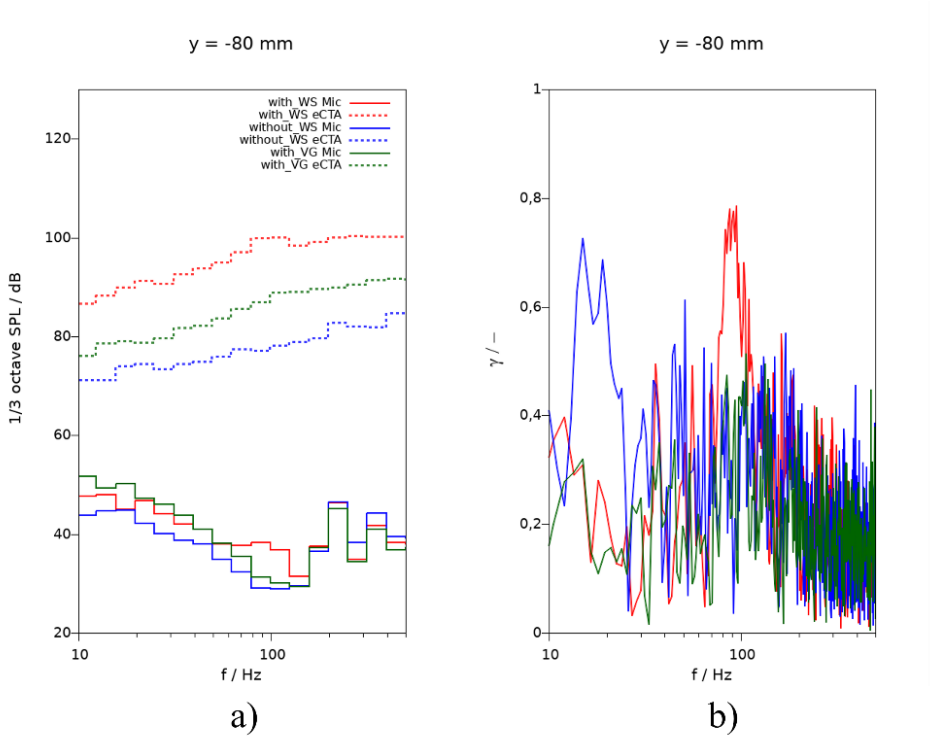

Figure 6: a) 1/3 octave sound pressure level frequency spectra and b) coherence function between hot-wire signal and microphone at y = - 80 mm of configurations *with_WS*, *without_WS* and *with_VG*

Figure 7 illustrates the distributions of the maximum sound pressure levels and coherence along the y-direction for the dominant frequency band associated with underbody buffeting (55 Hz < f < 110 Hz). It is important to note that high coherence does not necessarily correspond to large velocity fluctuation amplitudes, as coherence is derived from the cross-correlation function normalized by the autocorrelation functions of the two signals [9]. Rather, high coherence indicates a strong linear relationship between the two signals. This is evident when comparing Figures 7a) and 7b) of configuration *with_WS*. While coherence reaches its maximum in the fast main flow between the wheel spoilers, velocity fluctuations peak within the shear layer and decrease slightly towards the centre region. Figure 7b) further reveals a pronounced increase in coherence along the y-direction within the shear layer region, associated with dominant disturbance modes in the considered frequency range. These results highlight the crucial role of the shear layer in the development of buffeting.

Figure 7: a) Maximum sound pressure levels and b) coherence functions for frequency range 55 Hz < f < 110 Hz across the vehicle width of configurations *with_WS*, *without_WS* and *with_VG*

3.2 Configuration without wheel spoiler

This section discusses the configuration without wheel spoilers (*without_WS*), where no underbody buffeting occurs. The curves for this configuration are shown in blue in the diagrams.

First, the mean velocity profiles and standard deviation profiles of configurations *with_WS* and *without_WS* are compared (Figure 5). The position of the front wheel is indicated in the diagram between -200 mm < y < -150 mm. Downstream of the wheel, in the wake region, the flow velocity is significantly reduced in both cases, while between the wheels, the flow velocity approximately matches the free-stream velocity. Although both configurations exhibit a shear layer, buffeting occurs only in the *with_WS* case, as will be demonstrated. The configuration *without_WS* shows a strong velocity gradient around y ≈ -150 mm, whereas in the *with_WS* case, the shear layer is located further towards the vehicle centre at approximately y ≈ -100 mm. This shift is due to the wheel spoilers extending further towards the centerline. The thickness of a shear layer increases with its downstream length; since the hot-wire probe is positioned relatively close behind the front wheel, the shear layer behind the configuration *without_WS* is significantly narrower than that of the configuration *with_WS*.

Next, the 1/3 octave sound pressure level frequency spectra and the coherence function are examined (Figure 6). Comparing the hot-wire signals reveals that velocity fluctuations across the depicted frequency range are significantly lower in the configuration *without_WS* than in the configuration *with_WS*. Additionally, the differences in pressure fluctuations between the two configurations within the buffeting frequency range are considerably higher compared to other frequency ranges. Figure 6b) presents the coherence function calculated from the spectra shown on the left. A broad coherence peak is clearly visible within the buffeting frequency range of 55 Hz < f < 110 Hz. This peak is absent in the *without_WS* case (blue line). A peak observed in the 10 Hz < f < 25 Hz range is considered irrelevant due to the low amplitude levels in the signal. These results suggest that, without wheel spoilers, no acoustically significant flow structures occur in the considered case. When wheel spoilers are installed, a shear layer is formed where disturbance modes are amplified, causing underbody buffeting.

The frequency spectrum in Figure 7 clearly shows that velocity fluctuations, especially in the region between the wheels, are significantly lower for the configuration *without_WS* compared to the configuration *with_WS*. Similar amplitude levels in both hot-wire signals are observed only in the wake region of the wheels. This is because the fluctuating wake exhibits high levels across a wide frequency range, not limited to the shown bandwidth of 55 Hz < f < 110 Hz. Additionally, there is almost no correlation between the acoustic signals and the flow fluctuations measured by the hot-wire in the configuration *without_WS* (blue lines).

With installed wheel spoilers (*with_WS*, red), the amplitude measured by the microphone is significantly increased within the shown frequency range. The same applies to the fluctuations in the underbody flow field between the wheels. In this case, a strong coherence is observed. These two measurements clearly and quantitatively demonstrate that underbody buffeting occurs only when wheel spoilers are installed. The strongest correlations between sound signals measured inside the model and flow fluctuations beneath the vehicle are found in the region between the wheels. Disturbance modes within the shear layer separating the wake are strongly amplified, ultimately causing buffeting.

To gain additional insight into the flow field, the so-called kerosene soot technique was applied to visualize wall streamlines beneath the model. Figure 8 compares the flow patterns of the configurations *without_WS* and *with_WS*. Regions with high color density indicate areas where the oil accumulates due to low wall shear stress, whereas regions with less colour correspond to high wall shear stress caused by elevated flow velocities or strong velocity fluctuations resulting from intense turbulence. The shear layer regions exhibit high wall shear stress due to increased momentum exchange in the highly turbulent flow.

The baseline configuration *without_WS* (Figure 8a)) exhibits an almost homogeneous distribution of wall shear stress. In the configuration with wheel spoilers (Figure 8b)), two streaks of fluid accumulation form around the inner edge of the front wheel spoilers, separating the centre flow from the shear layer. The wake regions, which also contain the shear layers caused by the wheel spoilers, are identifiable by brighter areas where the oil paint has been strongly sheared off due to high skin friction. Within the shear layer separating the wakes from the mean flow between the wheels, disturbance modes are amplified, leading to low-frequency buffeting, as demonstrated by the quantitative measurements presented above. The shear layer position along the y-axis is further confirmed by the maximum standard deviation shown in Figure 5a).

a) b)

Figure 8: Wall shear patterns for the configurations a) *without_WS* and b) *with_WS*. Flow goes from left to right.

3.3 Configuration with vortex generator

From an aerodynamic perspective, wheel spoilers are essential components on the vehicle underbody to optimize the balance between drag and lift. The previous section demonstrated that wheel spoilers can induce buffeting, which is clearly perceptible in the passenger compartments of vehicles with flat underbodies (BEVs). The next step is to retain the spoilers while eliminating the buffeting.

By applying the various qualitative and quantitative methods presented above, the mechanism leading to underbody buffeting was identified. The disturbance modes originate from the shear layer developing around the inner edge of the wheel spoilers. Based on these findings, the goal was to modify the flow around the spoilers to prevent the formation of the unstable shear layer. The most straightforward approach is to generate a moderate vortex that suppresses the formation of an extensive wake (see Figure 8b)). This was achieved by a delta-shaped vortex generator adapted to the inner edge of the wheel spoiler. The longitudinal vortex prevents the formation of a large wake and its shear layer by enhancing momentum exchange along the model's underbody. As a result, pressure fluctuations caused by the shear layer are suppressed. The next section compares hot-wire measurement results and their correlation with those of the previously presented configurations *without_WS* and *with_WS*.

First, the mean velocity profiles and standard deviation profiles are considered. Figure 5 shows that the overall curve pattern for the configuration *with_VG* (green) is similar to that of the configuration *with_WS* (red). However, mean velocities in the wake region behind the wheel spoiler and wheel area have increased for the configuration *with_VG*, approaching values comparable to those in the *without_WS* case. The similarity between the configurations *with_WS* and *with_VG* arises because the mean values and standard deviations in Figure 5 encompass the entire frequency spectrum. To distinguish the different flow regimes of the *with_WS* and *with_VG* cases, it is essential to analyse the amplitude distributions in the frequency domain. Again, hot-wire results, their correlation with the microphone signal, and flow visualizations will demonstrate that the wake region behind the wheel spoilers behaves and appears significantly differently when combined with vortex generators compared to the original case with only wheel spoilers installed.

Next, the 1/3 octave frequency spectra and the coherence function between the acoustic and hot-wire signals are analyzed (Figure 6). Within the low-frequency range shown (0 Hz < f < 500 Hz), the amplitudes of the hot-wire signal are significantly reduced compared to configuration *with_WS*. Notably, underbody buffeting is completely suppressed, with amplitude levels comparable to the case *without_WS* and no buffeting. This suggests that the shear layer has been nearly eliminated, which may explain why the mean velocities in the wake of the configuration *with_VG* are approximately twice as high as those for configuration *with_WS*, as shown in Figure 5a).

Figure 5b) shows that in certain regions across the vehicle width, the standard deviation for configuration *with_VG* is significantly higher than for the case *without_WS*. Figure 6 reveals that these increased fluctuations are broadband, distributed across the entire frequency spectrum. The cause of the increased fluctuations is the vortex generator, which enhances momentum exchange. However, the interior microphone indicates that the relevant pressure fluctuations, especially within the underbody buffeting frequency range, are nearly as low as in the case *without_WS*. Consequently, the vortex generator reduces acoustically relevant velocity fluctuations and thus pressure fluctuations in the critical low-frequency range. This observation aligns with the coherence spectrum, where no significant correlations between velocity and pressure signals are detected across the relevant low-frequency range.

The hot-wire signal amplitudes in Figure 7 show a reduced level in the area between the wheels for the case *with_VG* (green) compared to the buffeting case (*with_WS*, red). Similarly, the pressure fluctuations inside the model are reduced to nearly the levels observed without underbody buffeting (*without_WS*, blue). Furthermore, the low maximum coherence values indicate no correlation between velocity fluctuations and the acoustic signal, confirming that the vortex generators effectively suppress underbody buffeting.

Figure 9 compares the visualized flow patterns for the configurations *with_WS* and *with_VG*. The formation of the unstable shear layer is clearly visible. In the *with_VG* case, the shear layer is significantly weakened by the longitudinal vortex generated by the vortex generator.

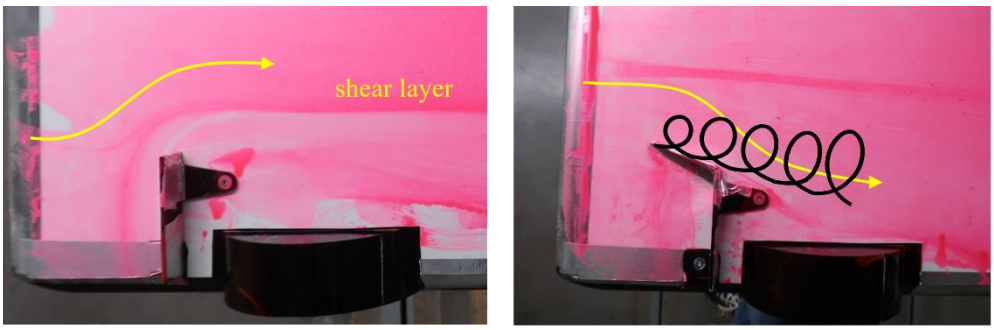

Figure 9: Soot visualizations of configuration a) *with_WS* and b) *with_VG*. Flow goes from left to right.

4 Conclusion

This paper investigates the underlying mechanism of the flow phenomenon "underbody buffeting." While previous studies employed extensive PIV measurements, this study utilizes a combined approach of hot-wire anemometry and microphones, integrated with real-time online evaluation, to demonstrate the direct relationship between measured flow fluctuations and their acoustic effects. The findings indicate that a strategic combination of various measurement methods provides deeper insights into the underlying mechanisms.

The measurements confirm that the disturbance modes, and thus the underbody buffeting, originate from the shear layer developing around the inner edge of the wheel spoilers. Subsequently, the measurement system was employed to develop a countermeasure against the buffeting by adapting a delta-shaped vortex generator to the inner edge of the wheel spoiler. The results show that this approach effectively reduces the high-pressure fluctuations. Additionally, the effectiveness and functioning of the vortex generators were visualized through the kerosene soot technique.

5 Acknowledgement

We gratefully acknowledge the Research Institute for Automotive Engineering and Powertrain Systems Stuttgart (FKFS) for the execution of the wind tunnel experiments. Furthermore, we would also like to acknowledge all our aerodynamics and aeroacoustics colleagues as well as the concept building team.

6 Bibliography

1. Helfer, M. “Umströmungsgeräusche“ from Hucho Aerodynamik des Automobils: Strömungsmechanik, Wärmetechnik, Fahrdynamik, Komfort,“ (München, Springer Vieweg, 2013), doi:10.1007/978-3-8348-2316-8.
2. Weber, C. “Aufbau einer aeroakustischen Simulationsmethode zur Bewertung der Fahrzeug-Unterbodenströmung,“ Master's thesis, Institute of Automotive Engineering, Stuttgart, 2018.
3. Staudenmayer, B. “Analyse der tieffrequenten Strömungsphänomene bei Fahrzeugen mit geschlossenem Unterboden,“ Master's thesis, Institute of Automotive Engineering, Stuttgart, 2021.
4. Breitenbücher, L., Wagner, A., Wiegand, T. and Brink, M., “Low Frequency Aerodynamic and Aeroacoustics Phenomena of Vehicles with Flat Underbody,“ presented at 13th FKFS Conference, Stuttgart, October 11-12, 2023.
5. Breitenbücher, L., Wagner, A., Wiegand, T., and Brink, M., “Experimental Investigation of Low-Frequency Flow Phenomena on the Vehicle Underbody Using Particle Image Velocimetry,” Tech. rep., SAE Technical Paper, 2024.
6. Breitenbücher, L., Wagner, A., Buderer, B., Wiegand, T., and Brink, M., “Identification of the Mechanism of Low Frequency Pressure Fluctuations Using Vortex Identification Methods,” AIAA/CEAS Aeroacoustics Conference 2024
7. Breitenbücher, L., Wagner, A., Wiegand, T., Brink, M., and Buderer, B., “Development of an Evaluation Methodology for PIV Measurements of Low-Frequency Flow Phenomena on the Vehicle Underbody,” Tech. rep., SAE Technical Paper, 2024.
8. AE Road Vehicle Aerodynamics Committee, “Aerodynamic Testing of Road Vehicles in Open Jet Wind Tunnel”, SAE Report J2071 (Open Throat Wind Tunnel Adjustments), Detroit, 2004
9. Bendat, J. S., & Piersol, A. G. (2010). Random Data: Analysis and Measurement Procedures (4th Edition). Wiley-Interscience.